Application of Filippov Theory to the IEEE Standard 421.5-2016 Anti-windup PI Controller

Mohammed Ahsan Adib Murad
School of Electrical & Electronic Eng.
University College Dublin (UCD)
Dublin, Ireland.
mohammed.murad@ucdconnect.ie

Brendan Hayes
School of Electronic Engineering
Dublin City University (DCU)
Dublin, Ireland.
brendan.hayes@dcu.ie

Federico Milano
School of Electrical & Electronic Eng.
University College Dublin (UCD)
Dublin, Ireland.
federico.milano@ucd.ie

***Abstract*—This paper applies the Filippov theory of differential equations with discontinuous right-hand side to model anti-windup PI controllers. The proposed approach solves the deadlock issue that arises in the PI control model recommended by the IEEE Standard 421.5-2016. An illustrative example as well as a case study based on a one-machine infinite-bus network show how the proposed approach works and discusses the effects of the proposed approach on the transient response of power systems.**

***Index Terms*—PI control, deadlock, anti-windup, Filippov theory, sliding surface.**

I. Introduction

A. Motivation

Proportional Integral (PI) controllers are commonly employed in power system applications [1]. The IEEE Standard 421.5-2016 is the recommended model. It proposes an anti-windup (AW) or non-windup PI control [2] model for dynamic analysis of power systems. The differential equation of this model is discontinuous. Due to discontinuity, simulations with the IEEE model can lead to failure of a numerical method or trajectory deadlock known as chattering Zeno [3]. This work applies Filippov theory (FT) to develop a method for the continuation of trajectories beyond such a deadlock point.

B. Literature Review

Integral windup phenomenon of PI controllers leads to excess energy to be dissipated in the system, which in turn results in a poor controller performance [4]. Thus AW control structures are often used and several solutions are proposed [5], [6]. Among all possible AW implementations, the definition of the IEEE Standard 421.5-2016 is a conditional integration type [2]. This IEEE AW model poses several challenges for both software implementation and numerical integration and one such issue is the deadlock.

The deadlock behavior that prevents the continuation of trajectories is discussed in [3] and [7] for PI controllers in wind turbines. To prevent such deadlock two approaches are proposed in [3], [7]: using an extra feedback loop and employing a deadband or hysteresis. The feedback solution has two disadvantages: it requires one extra parameter to be tuned and, depending on the disturbance, it can result in a significantly different dynamic behavior compared to the IEEE AW model as discussed in [1]. The application of the deadband approach introduces chattering of the solution on the discontinuous surface.

The breakdown of numerical integration techniques related to the IEEE AW model at the deadlock point is identified due to discretization in [8]. To alleviate this problem an auxiliary discrete variable based on the semi-implicit approach [9] is proposed in [8]. However, such semi-implicit formulation cannot be adopted by most power system simulation tools. Another technique considered in [8] is to employ a limited integrator. But this may result in a delayed response compared to the IEEE AW method. All the proposed methods mentioned above to overcome difficulties associated with the IEEE AW are based on *ad hoc* approaches. This work proposes a continuation technique based on FT [10].

Due to the conditions that dictate the non-smoothness of the IEEE AW model, the solution can enter into a constrained subset of the state space, typically known as *sliding* [11]. The formalism introduced by Filippov in [10] is a powerful tool to define a vector field on the sliding surface and to handle discontinuities. This has been applied in other fields, e.g., in power electronics [12]; and energy harvesters [13]. However, attempts to apply the FT to power system dynamic analysis have not been conducted thus far.

C. Contributions

The main contributions of the paper are as follows:

- The application of FT to the IEEE type AW PI control that leads to smooth continuation of trajectories.
- A comparison of the proposed approach with the approaches discussed in [3] and [8].

D. Organization

The remainder of this paper is organized as follows. Section II presents the IEEE Standard 421.5-2016 AW PI model along with the numerical issues associated with it. Section III introduces FT and explains its solution concept. A simple example of an AW PI controller with a time dependent input and a Single Machine Infinite Bus (SMIB) power system network are simulated by applying FT and compared with two existing solutions in Section IV. Finally, in Section V, conclusions and future work directions are drawn.

This work is supported by Science Foundation Ireland, by funding Mohammed Ahsan Adib Murad and Federico Milano, under Investigator Programme Grant No. SFI/15/IA/3074.

II. Problem Formulation

This section first presents the IEEE standard AW PI controller model and then illustrates the trajectory deadlock problem by introducing a relevant example.

A. Anti-windup PI control

The conditional integration AW method switches off the integration to avoid windup effects depending on certain conditions and there exists several implementations [5]. The IEEE standard proposes one of such AW method, depicted in Fig. 1. Mathematically, the model is [2]:

$$\begin{aligned} &\text{If } y \geqslant w_{\max} : w = w_{\max} \text{ and } \dot{x} = 0 \ , \\ &\text{If } y \leqslant w_{\min} : w = w_{\min} \text{ and } \dot{x} = 0 \ , \\ &\text{Otherwise} : w = y = k_p u + x \text{ and } \dot{x} = k_i u \ . \end{aligned} \tag{1}$$

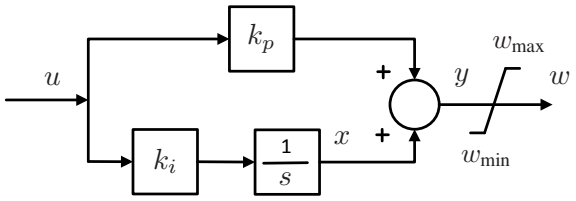

Fig. 1: Proportional-integral block with an anti-windup limiter in accordance with the IEEE Standard 421.5-2016 [2].

B. Numerical Issues of the IEEE Standard 421.5-2016

We use a simple example to explain the deadlock phenomenon that can occur when using the IEEE standard model. Let the following signal be the input signal to the PI controller:

$$\begin{aligned} \text{if } t < 3 \text{ then: } \dot{u} &= 1 \\ \text{else: } \dot{u} &= -1 \ , \end{aligned} \tag{2}$$

and the parameters considered are, $k_i = 3$, $k_p = 1$, $w_{\max} = 1.2$, $w_{\min} = -1.2$ and the initial values at $t = 0$ are $x_0 = 0.5$, and $u_0 = 0$. The system is simulated for 6.5 s with a time step 0.001 s.

Simulation results are shown in Fig. 2. The input u increases in the first 3 seconds of the simulation, hence y and w increase. For $y > w_{\max} = 1.2$, at $t = 0.427$ s w becomes constant and $\dot{x}$ switches to 0. So, the integrator is locked to prevent windup. For $t > 3$ s, u and y starts to decrease. At $t = 5.573$ s, $y < 1.2$ and the right-hand side of $\dot{x}$ unlocks. However, at the same time, $u > 0$ and, hence, $\dot{x} > 0$. Then x will increase, thus causing y to increase again towards $w_{\max}$. Depending on the time step of the integration and on the value of $\dot{x}$ and on the rate of change of the input u, a deadlock (cycling) situation can arise which consists in locking and unlocking the state variable x preventing the numerical integration from converging. Reducing the time step of the integration scheme does not solve this issue because of chattering at that discontinuous point. At this point, some kind of continuation process in necessary.

Using the deadband (db) based solution method with db = 0.003, the deadlock does not appear in the trajectory shown in Fig. 2. The db is implemented as in [3]. The trajectory obtained with the db model chatters between the bounds generated by the deadband and a reasonable value for db cannot be known as *a priori*.

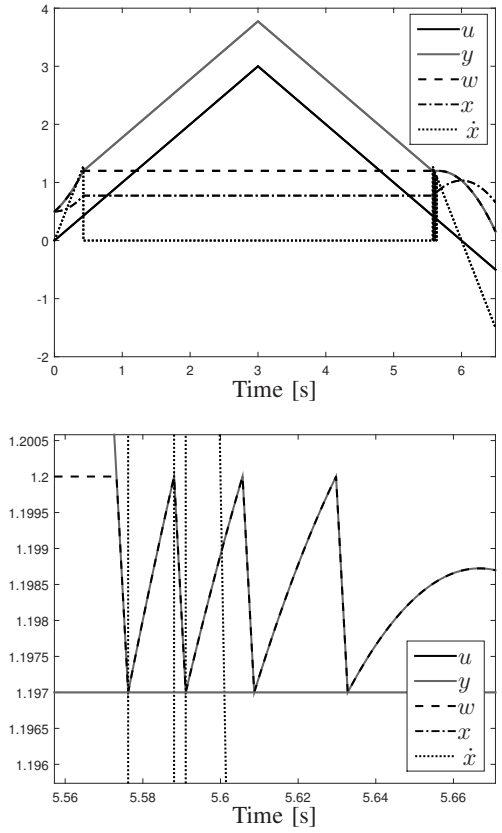

Fig. 2: An example to explain the deadlock phenomenon that occurs with the IEEE Standard 421.5-2016 anti-windup PI control model.

III. Filippov Theory

Filippov systems form a subclass of discontinuous dynamical systems which can be described by a set of first-order ordinary differential equations (ODEs) with a discontinuous right-hand side [10]. Consider the following switched dynamical system:

$$\dot{\boldsymbol{x}} = \boldsymbol{f}(\boldsymbol{x}) = \begin{cases} \boldsymbol{f_1}(\boldsymbol{x}) & \text{when } h(\boldsymbol{x}) < 0 \\ \boldsymbol{f_2}(\boldsymbol{x}) & \text{when } h(\boldsymbol{x}) > 0 \end{cases} \tag{3}$$

where, the event function $h : \mathbb{R}^n \to \mathbb{R}$ and an initial condition $\boldsymbol{x}(t_0) = \boldsymbol{x_0}$ are known.

The state space $\mathbb{R}^n$ is split into two regions R_1 and R_2 separated by a hyper-surface Σ where R_1, R_2 and Σ are characterized as,

$$\begin{aligned} R_1 &= \{\boldsymbol{x} \in \mathbb{R}^n \mid h(\boldsymbol{x}) < 0\}, \\ R_2 &= \{\boldsymbol{x} \in \mathbb{R}^n \mid h(\boldsymbol{x}) > 0\}, \\ \Sigma &= \{\boldsymbol{x} \in \mathbb{R}^n \mid h(\boldsymbol{x}) = 0\}, \end{aligned} \tag{4}$$

such that $\mathbb{R}^n = R_1 \cup \Sigma \cup R_2$, assuming that the gradient of h at $\boldsymbol{x} \in \Sigma$ never vanishes, $\boldsymbol{h_x}(\boldsymbol{x}) \neq \boldsymbol{0}$ for all $\boldsymbol{x} \in \Sigma$.

The vector field on Σ is defined by Filippov continuation approach, known as *Filippov convex method* [10]. This method states that the vector field on the surface of discontinuity is a convex combination of the two vector fields in the different regions of the state-space:

$$\dot{\boldsymbol{x}} = \boldsymbol{f}(\boldsymbol{x}) = \begin{cases} \boldsymbol{f_1}(\boldsymbol{x}), & \boldsymbol{x} \in R_1 \\ \overline{co}\{\boldsymbol{f_1}(\boldsymbol{x}), \boldsymbol{f_2}(\boldsymbol{x})\}, & \boldsymbol{x} \in \Sigma \\ \boldsymbol{f_2}(\boldsymbol{x}), & \boldsymbol{x} \in R_2 \end{cases} \tag{5}$$

where, $\overline{co}(\boldsymbol{f_1}, \boldsymbol{f_2})$ is the minimal closed convex set containing $\boldsymbol{f_1}$ and $\boldsymbol{f_2}$, i.e.

$$\overline{co}\{\boldsymbol{f_1}, \boldsymbol{f_2}\} = \{\boldsymbol{f}_F : \boldsymbol{x} \in \mathbb{R}^n \to \mathbb{R}^n : \boldsymbol{f}_F = (1-\alpha)\boldsymbol{f}_1 + \alpha \boldsymbol{f}_2\}, \tag{6}$$

where $\alpha \in [0, 1]$.

Definition 1: An absolutely continuous function $\boldsymbol{x} : [\boldsymbol{0}, \boldsymbol{\tau}] \to \mathbb{R}^n$ is said to be a solution of (3) in the sense of Filippov, if for almost all $t \in [\boldsymbol{0}, \boldsymbol{\tau}]$ it holds that

$$\dot{\boldsymbol{x}} \in \boldsymbol{F}(\boldsymbol{x}(t))$$

where $\boldsymbol{F}(\boldsymbol{x}(t))$ is close convex hull in (6).

Now, the question is what happens when the trajectory of $\dot{\boldsymbol{x}} = \boldsymbol{f_1}(\boldsymbol{x}),$ with $\boldsymbol{x}(\boldsymbol{0}) = \boldsymbol{x_0}$ reaches at Σ in finite time. The possibilities are: (a) transversal crossing, (b) attractive sliding or repulsive sliding and (c) smooth exit. Filippov formulated a first order theory to decide what to do in such kind of situation, summarized in the following.

A. Filippov First Order Theory

Filippov first order theory defines the vector field if the solution approaches the discontinuous surface. Let $\boldsymbol{x} \in \Sigma$ and $\boldsymbol{n}(\boldsymbol{x})$ is the unit normal to Σ at $\boldsymbol{x}$ i.e. $\boldsymbol{n}(\boldsymbol{x}) = \frac{\boldsymbol{h_x}(\boldsymbol{x})}{\|\boldsymbol{h_x}(\boldsymbol{x})\|}$ where, $\boldsymbol{h_x}(\boldsymbol{x}) = \nabla h(\boldsymbol{x})$ and $\nabla = \frac{\partial}{\partial \boldsymbol{x}}$; the components of $\boldsymbol{f_1}(\boldsymbol{x})$ and $\boldsymbol{f_2}(\boldsymbol{x})$ onto the normal to the Σ are $\boldsymbol{n}^T(\boldsymbol{x})\boldsymbol{f_1}(\boldsymbol{x})$ and $\boldsymbol{n}^T(\boldsymbol{x})\boldsymbol{f_2}(\boldsymbol{x})$ respectively.

1) Transversal Crossing: If at $\boldsymbol{x} \in \Sigma$,

$$(\boldsymbol{n}^T(\boldsymbol{x})\boldsymbol{f_1}(\boldsymbol{x})).(\boldsymbol{n}^T(\boldsymbol{x})\boldsymbol{f_2}(\boldsymbol{x})) > 0, \tag{7}$$

the trajectory leaves Σ, and two cases are possible. The system will move to R_2 with $\boldsymbol{f} = \boldsymbol{f_2}$, if $\boldsymbol{n}^T(\boldsymbol{x})\boldsymbol{f_1}(\boldsymbol{x}) > 0$ or it will enter to R_1 with $\boldsymbol{f} = \boldsymbol{f_1}$, if $\boldsymbol{n}^T(\boldsymbol{x})\boldsymbol{f_1}(\boldsymbol{x}) < 0$.

2) Sliding mode: Sliding occurs, at $\boldsymbol{x} \in \Sigma$ if,

$$(\boldsymbol{n}^T(\boldsymbol{x})\boldsymbol{f_1}(\boldsymbol{x})).(\boldsymbol{n}^T(\boldsymbol{x})\boldsymbol{f_2}(\boldsymbol{x})) < 0\ . \tag{8}$$

The sliding mode can be an attracting or a repulsive one. An attracting sliding mode will occur if,

$$(\boldsymbol{n}^T(\boldsymbol{x})\boldsymbol{f_1}(\boldsymbol{x})) > 0 \quad \text{and} \quad (\boldsymbol{n}^T(\boldsymbol{x})\boldsymbol{f_2}(\boldsymbol{x})) < 0,\ \boldsymbol{x} \in \Sigma. \tag{9}$$

Repulsive sliding falls outside the scope of this work. Interested readers are pointed to [10] for further details of this form of sliding. While sliding along Σ, time derivative $\boldsymbol{f}_F$ is given by:

$$\boldsymbol{f}_F(\boldsymbol{x}) = (1-\alpha(\boldsymbol{x}))\boldsymbol{f_1}(\boldsymbol{x}) + \alpha(\boldsymbol{x})\boldsymbol{f_2}(\boldsymbol{x}), \tag{10}$$

where, $\alpha(\boldsymbol{x})$ is given by [proof, see [10]]:

$$\alpha(\boldsymbol{x}) = \frac{\boldsymbol{n}^T(\boldsymbol{x})\boldsymbol{f_1}(\boldsymbol{x})}{\boldsymbol{n}^T(\boldsymbol{x})(\boldsymbol{f_1}(\boldsymbol{x}) - \boldsymbol{f_2}(\boldsymbol{x}))}\ . \tag{11}$$

The sliding mode continues until one of the vector fields starts to point away. When this happens, the solution can be continued above or below the sliding surface. The exit point is calculated numerically by finding either the root $\alpha(\boldsymbol{x}) = 0$ or $\alpha(\boldsymbol{x}) = 1$ as appropriate. The following remarks are relevant:

- *If $\boldsymbol{f}_F(\boldsymbol{x}) \neq \boldsymbol{f_1}(\boldsymbol{x})$, $\boldsymbol{f}_F(\boldsymbol{x}) \neq \boldsymbol{f_2}(\boldsymbol{x})$ such a solution is often called a sliding motion.*
- A solution having an attractive sliding mode exists and is unique, in forward time.
- If at the point of discontinuity, condition (8) becomes $\leqslant 0$ and $\boldsymbol{f_1}(\boldsymbol{x}) \neq \boldsymbol{f_2}(\boldsymbol{x})$ then a continuous vector-valued function $\boldsymbol{f}_F(\boldsymbol{x})$ is given which determines the velocity of motion $\dot{\boldsymbol{x}} = \boldsymbol{f}_F(\boldsymbol{x})$ along the discontinuity line. If $\boldsymbol{n}^T(\boldsymbol{x})\boldsymbol{f_1}(\boldsymbol{x}) = 0$ then $\boldsymbol{f}_F(\boldsymbol{x}) = \boldsymbol{f_1}(\boldsymbol{x})$; if $\boldsymbol{n}^T(\boldsymbol{x})\boldsymbol{f_2}(\boldsymbol{x}) = 0$ then $\boldsymbol{f}_F(\boldsymbol{x}) = \boldsymbol{f_2}(\boldsymbol{x})$.

IV. Case Study

In order to demonstrate the application of Filippov theory on IEEE AW PI controller two case studies are considered. The first case study re-calls the example from Section II-B and the second one considers an SMIB power system network. The algorithm described in [14] is applied for numerical simulation.

A. Case Study I

Consider the example discussed in Section II-B with the same input and parameters. The mathematical model for upper limit becomes:

$$\dot{\boldsymbol{x}} = \boldsymbol{f}(\boldsymbol{x}) = \begin{cases} \boldsymbol{f_1}(\boldsymbol{x}) = \boldsymbol{f_{ns}} = \begin{bmatrix} \dot{u} \\ k_i x_1 \end{bmatrix} & \text{when } h(\boldsymbol{x}) < 0 \\ \boldsymbol{f_2}(\boldsymbol{x}) = \boldsymbol{f_s} = \begin{bmatrix} \dot{u} \\ 0 \end{bmatrix} & \text{when } h(\boldsymbol{x}) > 0, \end{cases}$$

where $\boldsymbol{f_{ns}}$ and $\boldsymbol{f_s}$ are the differential equations when the controller is not saturated and saturated, respectively and u varies according to (2). The controller output signal $y = k_p x_1 + x_2$. The switching manifold is given by: $h(\boldsymbol{x}) = y - 1.2$. So, $\boldsymbol{h_x}(\boldsymbol{x}) = [\frac{\partial h(\boldsymbol{x})}{\partial x_1} \quad \frac{\partial h(\boldsymbol{x})}{\partial x_2}]^T = [k_p \quad 1]^T$, and the normal to the switching surface is: $\boldsymbol{n}^T(\boldsymbol{x}) = [k_p \quad 1]$.

The simulation results are shown in Fig. 3 and how FT is applied at each discontinuous point described below.

- $t = 0$ (s): With initial conditions $[0; 0.5]$, $h(\boldsymbol{x}) < 0$, thus the system starts in the non-saturated region and is modeled with $\boldsymbol{f} = \boldsymbol{f_{ns}}$.
- $t = 0.4268$ (s): The system has struck the switching manifold i.e. $h(\boldsymbol{x}) = 0$ with $u = 0.4268$. At the switching surface, calculating,

$$\boldsymbol{n}^T(\boldsymbol{x})\boldsymbol{f_1}(\boldsymbol{x}) = [1 \quad 1] \begin{bmatrix} 1 \\ 3(0.4268) \end{bmatrix} = 2.2804$$

$$\boldsymbol{n}^T(\boldsymbol{x})\boldsymbol{f_2}(\boldsymbol{x}) = [1 \quad 1] \begin{bmatrix} 1 \\ 0 \end{bmatrix} = 1$$

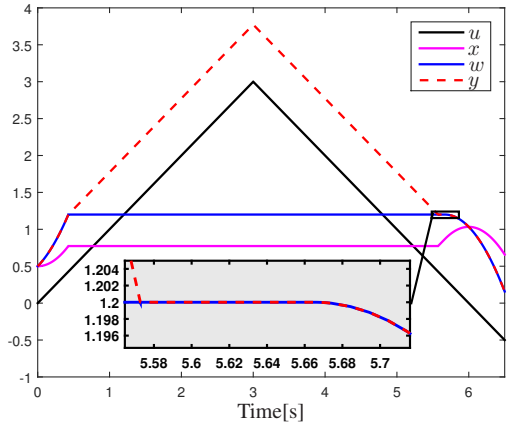

Fig. 3: Response of trajectories using Filippov theory.

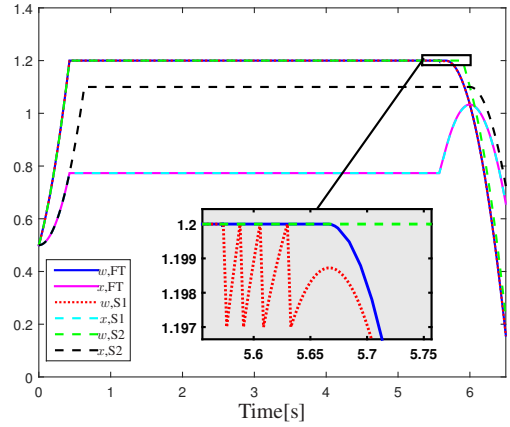

Fig. 4: Comparision of trajectories using Filippov theory (FT), deadband approach (S1) and limited integrator technique (S2).

The system undergoes a transversal intersection since $[\boldsymbol{n}^T(\boldsymbol{x})\boldsymbol{f_1}(\boldsymbol{x})].[\boldsymbol{n}^T(\boldsymbol{x})\boldsymbol{f_2}(\boldsymbol{x})] = 2.2804 > 0$. Since $\boldsymbol{n}^T(\boldsymbol{x})\boldsymbol{f_1}(\boldsymbol{x}) > 0$, the system moves region with $\boldsymbol{f} = \boldsymbol{f_s}$.

- $t = 3$ (s): a time dependent switching occurs, exactly at that moment for $\dot{u} = -1$, and $h(\boldsymbol{x}) > 0$ so, the system continues with $\boldsymbol{f} = \boldsymbol{f_s}$. For values of t greater than 3, the input signal now starts to decrease.
- $t = 5.5728$ (s): The system has again struck the switching manifold with $u = 0.4268$. At this point, calculating,

$$\boldsymbol{n}^T(\boldsymbol{x})\boldsymbol{f_1}(\boldsymbol{x}) = [1 \quad 1]\begin{bmatrix} -1 \\ 3(0.4268) \end{bmatrix} = 0.2804$$
$$\boldsymbol{n}^T(\boldsymbol{x})\boldsymbol{f_2}(\boldsymbol{x}) = [1 \quad 1]\begin{bmatrix} -1 \\ 0 \end{bmatrix} = -1 \ .$$

$[\boldsymbol{n}^T(\boldsymbol{x})\boldsymbol{f_1}(\boldsymbol{x})].[\boldsymbol{n}^T(\boldsymbol{x})\boldsymbol{f_2}(\boldsymbol{x})] = -0.2804 < 0$ and according to (9), the system slides along Σ. Next, the sliding vector field on Σ is calculated using (10,11):

$$\alpha(\boldsymbol{x}) = \frac{\boldsymbol{n}^T(\boldsymbol{x})\boldsymbol{f_1}(\boldsymbol{x})}{\boldsymbol{n}^T(\boldsymbol{x})(\boldsymbol{f_1}(\boldsymbol{x}) - \boldsymbol{f_2}(\boldsymbol{x}))} = \frac{3u-1}{3u}$$
$$\boldsymbol{f}_F(\boldsymbol{x}) = (1-\alpha(\boldsymbol{x}))\boldsymbol{f_1}(\boldsymbol{x}) + \alpha(\boldsymbol{x})\boldsymbol{f_2}(\boldsymbol{x})$$
$$= \begin{bmatrix} x_1 \\ x_2 \end{bmatrix} = \begin{bmatrix} -1 \\ 1 \end{bmatrix} \ .$$

- $t = 5.6663$ (s): At this point, $\alpha(\boldsymbol{x}) = 0$ for $u = \frac{1}{3}$ and the trajectory leaves Σ with vector field $\boldsymbol{f_{ns}}$.

1) Comparison of Solutions: This section compares the Filippov solution approach with the db solution method and the limited integration technique (LIT). The limited integrator [8] model is as follows:

$$\begin{aligned} &\text{If } y \geqslant w_{\max} : w = w_{\max} \ , \\ &\text{If } y \leqslant w_{\min} : w = w_{\min} \ , \\ &\text{Otherwise} : w = y = k_p u + x \ , \end{aligned} \tag{12}$$

$$\begin{aligned} &\text{If } x \geqslant x_{\max} \text{ and } \dot{x} \geqslant 0 \ : x = x_{\max} \text{ and } \dot{x} = 0 \ , \\ &\text{If } x \leqslant x_{\min} \text{ and } \dot{x} \leqslant 0 \ : x = x_{\min} \text{ and } \dot{x} = 0 \ , \\ &\text{Otherwise} : \dot{x} = k_i u \ . \end{aligned} \tag{13}$$

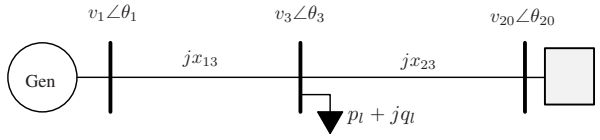

Fig. 5: A single generator connected to an infinite bus.

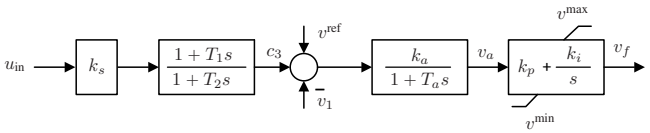

Fig. 6: Block diagram of AVR and PSS.

The db value used is 0.003 and the integrator is limited ± 1.1 for LIT. The simulation results are shown in Fig. 4. Using FT and LIT the trajectory continues smoothly before and after each event; the db approach will always results in chattering whenever a deadlock condition appears.

On the other hand, LIT does not show the deadlock and provides some flexibility to choose the integrator limits independently. However, correct values for limits of the integrator state are often unknown and a common choice is to use the same values as the output limit. Therefore, in most of the situations using LIT compared to FT and db, will result in a different convergence rate to steady state after the output leaves the limit.

B. Case Study II

Consider the SMIB system shown in Fig. 5, the generator is equipped with an Automatic Voltage Regulator (AVR) and a Power System Stabilizer (PSS) as depicted in Fig. 6. The generator model is a third order type; the PSS consists of a stabilizer gain and a lead lag block and the AVR is an static type with PI control [15]. The dynamics of the system is described by a set of differential-algebraic equations (DAEs)

in the following form [15],

$$\begin{aligned} \dot{\boldsymbol{x}} &= \boldsymbol{f}(\boldsymbol{x}, \boldsymbol{y}) \ , \\ \boldsymbol{0} &= \boldsymbol{g}(\boldsymbol{x}, \boldsymbol{y}) \ , \end{aligned} \tag{14}$$

where $\boldsymbol{x}$ and $\boldsymbol{y}$ are the vector of state and algebraic variables respectively.

For this test system, $\boldsymbol{x} = [\delta \ \omega \ e'_q \ v_a \ x_i \ s_1]^T$, $\boldsymbol{y} = [v_1 \ v_3 \ \theta_1 \ \theta_3 \ v_f \ c_1 \ c_2 \ c_3]^T$, where δ, ω, e'_q are the rotor angle, rotor speed and q-axis transient voltage respectively; v_a, x_i and s_1 are the state variables of AVR and PSS; v_1, v_3, θ_1, θ_3 are the bus voltages and angles respectively; v_f is the generator field voltage; c_1, c_2, c_3 are the algebraic variables of PSS.

The algebraic equations of the SMIB system are given by,

$$\begin{aligned} 0 &= -p_e + b_{13} v_1 v_3 \sin(\theta_1 - \theta_3) \ , \\ 0 &= b_{13} v_3 v_1 \sin(\theta_3 - \theta_1) + b_{23} v_3 \sin(\theta_3) + p_l \ , \\ 0 &= -q_e + b_{13}[v_1^2 - v_1 v_3 \cos(\theta_1 - \theta_3)] \ , \\ 0 &= b_{13}[v_3^2 - v_3 v_1 \cos(\theta_3 - \theta_1)] + b_{23}[v_3^2 - v_3 \cos(\theta_3)] + q_l \ , \\ 0 &= -v_f + k_p v_a + x_i \ , \\ 0 &= c_1 - u_{\text{in}} k_s \ , \\ 0 &= c_2 - c_1(1 - \frac{T_1}{T_2}) \ , \\ 0 &= c_3 - c_1(\frac{T_1}{T_2}) - s_1 \ , \end{aligned}$$

where $b_{13} = 1/x_{13}$ and $b_{23} = 1/x_{23}$ are known line parameters; k_p, k_s, T_1 and T_2 are the control parameters of AVR and PSS; input to the PSS is $u_{\text{in}} = \omega$; $p_l = p_{l0}(\frac{v_3}{v_{30}})$, $q_l = q_{l0}(\frac{v_3}{v_{30}})^2$, v_{30} is known from power flow calculation; p_{l0} and q_{l0} are the active and reactive power of the load respectively; the reactive and active power of the generator are: $q_e = -\frac{1}{x'_d}[v_1^2 - e'_q v_1 \cos(\theta_1 - \delta_1)]$, $p_e = \frac{e'_q v_1}{x'_d} \sin(\delta - \theta_1)$ respectively. Note that, the voltage and angle of the infinite bus are $v_{20} = 1$ and $\theta_{20} = 0$ respectively.

The PI controller in AVR (see Fig. 6) is an IEEE Standard 421.5-2016 type. Lets consider the switching manifold for an upper limit, $h(\boldsymbol{x}) = k_p v_a + x_i - v^{\max}$. When $h(\boldsymbol{x}) < 0$, the differential equations of the SMIB system are given by ,

$$\dot{\delta} = \omega \tag{15}$$

$$\dot{\omega} = \frac{1}{M}(p_m - p_e - D\omega) \tag{16}$$

$$\dot{e}'_q = \frac{1}{T'_{d0}}(v_f - \frac{x_d}{x'_d} e'_q + \frac{x_d - x'_d}{x'_d} v_1 \cos(\delta - \theta_1)) \tag{17}$$

$$\dot{v}_a = (k_a(v^{\text{ref}} + c_3 - v_1) - v_a)/T_a \tag{18}$$

$$\dot{x}_i = k_i v_a \tag{19}$$

$$\dot{s}_1 = \frac{1}{T_2}(c_2 - s_1) \ , \tag{20}$$

where x_d, x'_d are the d-axis synchronous and transient reactance respectively; T'_{d0}, M, D and p_m are the d-axis open circuit transient time constant, the mechanical starting time, the damping coefficient and the mechanical power input to the generator respectively; v^{ref} is the reference voltage; T_a, k_i and k_a are the control parameters of AVR and PSS.

TABLE I
PARAMETERS OF THE COMPONENTS OF THE SMIB NETWORK

Name	Values
Generator	$M = 8$, $D = 0$, $x'_d = 0.25$, $x_d = 1$, $p_m = 1$, $T'_{d0} = 6$
Line	$x_{13} = 0.3$, $x_{23} = 0.5$
Load	$p_{l0} = 0.7$, $q_{l0} = 0.01$
AVR	$k_a = 2$, $T_a = 0.005$, $k_p = 5.5$, $k_i = 35$, $v^{\max} = 1.58$, $v^{\min} = -1.5$, $v^{\text{ref}} = 1$
PSS	$k_s = 1.5$, $T_1 = 0.23$, $T_2 = 0.12$

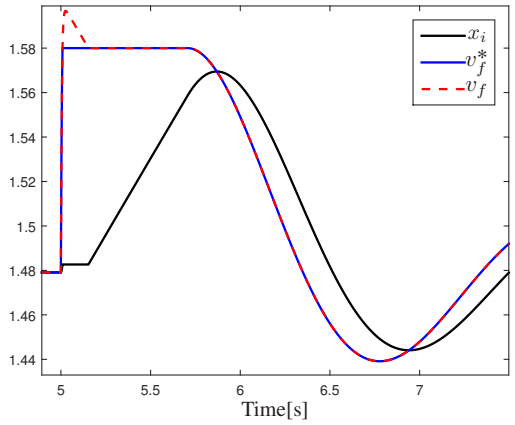

Fig. 7: Response of the state and field voltage using Filippov theory.

When $h(\boldsymbol{x}) > 0$ i.e. the field voltage reaches to its upper limit ($v^{\max}$) then (17) and (19) will be switched and all other states will remain same, as follows:

$$\dot{e}'_q = \frac{1}{T'_{d0}}(v^{\max} - \frac{x_d}{x'_d} e'_q + \frac{x_d - x'_d}{x'_d} v_1 \cos(\delta - \theta_1)) \tag{21}$$

$$\dot{x}_i = 0 \tag{22}$$

We consider $\boldsymbol{f_1}(\boldsymbol{x}, \boldsymbol{y})$ is (15)-(20) and $\boldsymbol{f_2}(\boldsymbol{x}, \boldsymbol{y})$ is (15), (16), (21), (18), (22) and (20). Calculating, $\boldsymbol{h_x}(\boldsymbol{x}) = [\frac{\partial h(\boldsymbol{x})}{\partial x_1} \ \ \frac{\partial h(\boldsymbol{x})}{\partial x_2} \ \ \ldots \ \ \frac{\partial h(\boldsymbol{x})}{\partial x_6}]^T = [0 \ 0 \ 0 \ k_p \ 1 \ 0]^T$, and the normal to the switching surface is: $\boldsymbol{n}^T(\boldsymbol{x}) = [0 \ 0 \ 0 \ k_p \ 1 \ 0]$.

The initial values of the state variables and algebraic variables are calculated from the power flow solution and are: $\boldsymbol{x_0} = [\delta_0 \ \omega_0 \ e'_{q0} \ v_{a0} \ x_{i0} \ s_{10}]^T = [0.702 \ 0 \ 1.10 \ 0 \ 1.478 \ 0]^T$, $\boldsymbol{y_0} = [v_{10} \ v_{30} \ \theta_{10} \ \theta_{30} \ v_{f0} \ c_{10} \ c_{20} \ c_{30}]^T = [1 \ 0.962 \ 0.473 \ 0.156 \ 1.478 \ 0 \ 0 \ 0]^T$. All the parameters of different components of the SMIB system are given in Table I.

1) Simulation Results: The SMIB test system is simulated by applying a step increase to load ($p_{l0} = 0.701, q_{l0} = 0.015$) and voltage reference set-point of AVR ($v^{\text{ref}} = 1.01$) at 5 s. The response of the PI controller state, field voltage and limited field voltage (v_f^*) using FT are shown in Fig. 7. To explain how FT is applied during each event, $h(\boldsymbol{x})$; $r_1 = \boldsymbol{n}^T(\boldsymbol{x})\boldsymbol{f_1}(\boldsymbol{x}, \boldsymbol{y})$ and $r_2 = \boldsymbol{n}^T(\boldsymbol{x})\boldsymbol{f_2}(\boldsymbol{x}, \boldsymbol{y})$ are shown in Fig. 8. Simulation results clearly show that a piece-wise smooth solution is achieved using Filippov solution technique. Relevant remarks on the simulation results are given below:

- For the initial operating point of the system $h(\boldsymbol{x}) < 0$, so the system simulation starts with $\boldsymbol{f_1}(\boldsymbol{x}, \boldsymbol{y})$.

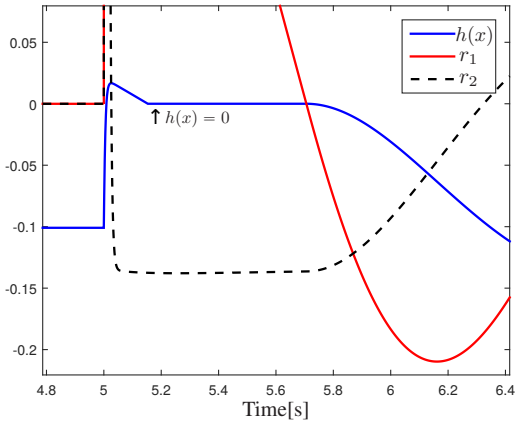

Fig. 8: Response of the switching manifold $h(\boldsymbol{x})$, $r_1 = \boldsymbol{n}^T(\boldsymbol{x})\boldsymbol{f_1}(\boldsymbol{x},\boldsymbol{y})$ and $r_2 = \boldsymbol{n}^T(\boldsymbol{x})\boldsymbol{f_2}(\boldsymbol{x},\boldsymbol{y})$ using Filippov theory.

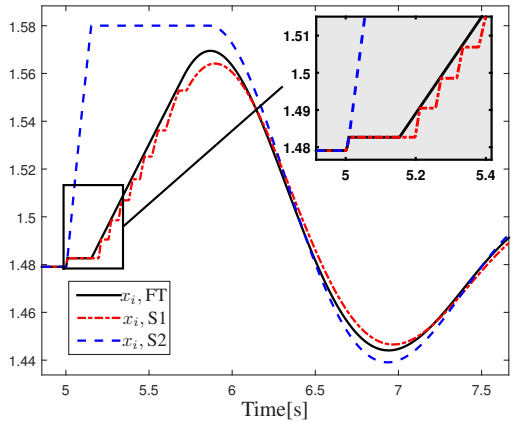

Fig. 9: Comparision of trajectories using Filippov theory (FT), deadband approach (S1) and limited integrator technique (S2).

- At 5 s the disturbance is applied and a little bit after that the system reaches to the switching manifold i.e. $h(\boldsymbol{x}) = 0$. Due to the condition (7) and $r_1 > 0$ (see Fig. 8) a transversal crossing is happened. The system switches to $\boldsymbol{f_2}(\boldsymbol{x},\boldsymbol{y})$ and the integrator state and the field voltage become constant (see Fig. 7). The system continues with $\boldsymbol{f_2}(\boldsymbol{x},\boldsymbol{y})$ as long as $h(\boldsymbol{x}) > 0$.
- At $t = 5.153$ s, $h(\boldsymbol{x}) = 0$ again (see the arrow in Fig. 8) and the conditions (8) and (9) are met, so an attracting sliding mode occurs on $h(\boldsymbol{x}) = 0$. The vector field ($\boldsymbol{f}_F(\boldsymbol{x},\boldsymbol{y})$) and $\alpha(\boldsymbol{x},\boldsymbol{y})$ are calculated numerically using (10) and (11). Therefore during that sliding $h(\boldsymbol{x})$ remains at 0, the system continues with $\boldsymbol{f}_F(\boldsymbol{x},\boldsymbol{y})$ (see Figs. 7-8).
- The system moves to $\boldsymbol{f_1}(\boldsymbol{x},\boldsymbol{y})$ when $h(\boldsymbol{x}) < 0$.

The theory of Filippov assumes systems are modeled using ODEs. However in this work, our system model employs DAEs to simulate power systems. The application of FT was possible due to the fact that $h(\boldsymbol{x})$ depended only on the state variables and not the algebraic ones. In addition, the case studies shows the effectiveness of FT for upper limit of the IEEE AW PI controller but it is trivial to apply for lower limit too. For completeness Fig. 9 compares the db and LIT with the FT (only the integrator state is shown).

V. Conclusions

This paper studies the trajectory deadlock issue of the IEEE Standard 421.5-2016 AW PI controller model. To solve this deadlock problem Filippov theory is proposed. The case studies prove that an effective trajectory continuation can be achieved using convex combination defined by Filippov. Other alternative solution techniques were also compared with the FT.

We are currently actively working on implementing a systematic formulation of the FT in a software tool for power system analysis. We believe that the results of this paper are promising. However there is still much research to do to make FT suitable for commercial grade software tools. In particular, we aim at studying how to apply FT to systems where $h(\boldsymbol{x},\boldsymbol{y})$ depends on both state and algebraic variables.

References

[1] M. A. A. Murad, Á. Ortega, and F. Milano, "Impact on power system dynamics of PI control limiters of VSC-based devices," in *Power Systems Computation Conference (PSCC)*, June 2018, pp. 1–7.

[2] "IEEE recommended practice for excitation system models for power system stability studies - redline," *IEEE Std 421.5-2016 (Revision of IEEE Std 421.5-2005) - Redline*, pp. 1–453, Aug 2016.

[3] I. A. Hiskens, "Dynamics of type-3 wind turbine generator models," *IEEE Transactions on Power Systems*, vol. 27, no. 1, pp. 465–474, Feb 2012.

[4] K. J. Åström and T. Hägglund, *Advanced PID Control*. ISA - The Instrumentation, Systems and Automation Society, 2006.

[5] A. Visioli, "Modified anti-windup scheme for PID controllers," *IEE Proceedings - Control Theory and Applications*, vol. 150, no. 1, pp. 49–54, Jan 2003.

[6] S. Tarbouriech and M. Turner, "Anti-windup design: an overview of some recent advances and open problems," *IET Control Theory Applications*, vol. 3, no. 1, pp. 1–19, January 2009.

[7] I. A. Hiskens, "Trajectory deadlock in power system models," in *2011 IEEE International Symposium of Circuits and Systems (ISCAS)*, May 2011, pp. 2721–2724.

[8] D. Fabozzi, S. Weigel, B. Weise, and F. Villella, "Semi-implicit formulation of proportional-integral controller block with non-windup limiter according to IEEE Standard 421.5-2016," in *Bulk Power Systems Dynamics and Control Symposium (IREP)*, 2017, pp. 1–7.

[9] F. Milano, "Semi-implicit formulation of differential-algebraic equations for transient stability analysis," *IEEE Transactions on Power Systems*, vol. 31, no. 6, pp. 4534–4543, Nov 2016.

[10] A. F. Filippov, *Differential Equations with Discontinuous Righthand Sides*. Kluwer Academic Publishers, 1988.

[11] M. di Bernardo, P. Kowalczyk, and A. Nordmark, "Bifurcations of dynamical systems with sliding: derivation of normal-form mappings," *Physica D: Nonlinear Phenomena*, vol. 170, no. 3, pp. 175 – 205, 2002.

[12] D. Giaouris, S. Banerjee, B. Zahawi, and V. Pickert, "Stability analysis of the continuous-conduction-mode buck converter via Filippov's method," *IEEE Transactions on Circuits and Systems I: Regular Papers*, vol. 55, no. 4, pp. 1084–1096, May 2008.

[13] P. Harte, E. Blokhina, O. Feely, D. Fournier-Prunaret, and D. Galayko, "Electrostatic vibration energy harvesters with linear and nonlinear resonators," *International Journal of Bifurcation and Chaos*, vol. 24, no. 11, p. 1430030, 2014.

[14] P. T. Piiroinen and Y. A. Kuznetsov, "An event-driven method to simulate Filippov systems with accurate computing of sliding motions," *ACM Trans. Math. Softw.*, vol. 34, no. 3, pp. 13:1–13:24, May 2008.

[15] F. Milano, *Power System Modelling and Scripting*, ser. Power Systems. Springer Berlin Heidelberg, 2010.